

## FAST TRACK COMMUNICATION

# Electronic transport properties of charge-ordered $\text{Bi}_{0.4}\text{Ca}_{0.6}\text{MnO}_3$ film

Y Z Chen, J R Sun<sup>1</sup>, D J Wang, S Liang, J Z Wang, Y N Han, B S Han  
and B G Shen

Institute of Physics and Beijing National Laboratory for Condensed Matter Physics,  
Chinese Academy of Sciences, Beijing 100080, People's Republic of China

E-mail: [jrsun@g203.iphy.ac.cn](mailto:jrsun@g203.iphy.ac.cn)

Received 29 August 2007, in final form 28 September 2007

Published 16 October 2007

Online at [stacks.iop.org/JPhysCM/19/442001](http://stacks.iop.org/JPhysCM/19/442001)

## Abstract

The electronic transport properties of charge-ordered  $\text{Bi}_{0.4}\text{Ca}_{0.6}\text{MnO}_3$  films grown on a (110)  $\text{SrTiO}_3$  substrate are experimentally studied. Special attention has been paid to the Hall effect around the charge-ordering (CO) transition. The charge carriers are found to be electron-like, and the carrier density  $n$  exhibits a significant change upon the CO transition: it is nearly constant above the transition temperature  $T_{\text{co}}$ ,  $\sim 0.36$  electrons/Mn, and reduces with decrease of the temperature below  $T_{\text{co}}$  following the formula  $n \propto \exp(-E_{\text{H}}/k_{\text{B}}T)$ , with an activation energy  $E_{\text{H}}$  of  $\sim 0.13$  eV. In contrast, no obvious signatures of thermal activation for Hall mobility were observed. Meanwhile, it is revealed that magnetic field affects the resistivity by enhancing the carrier mobility of the film in the course of the CO transition.

Charge ordering (CO), i.e. a periodic arrangement of  $\text{Mn}^{3+}$  and  $\text{Mn}^{4+}$  below a critical temperature  $T_{\text{co}}$ , is one of the most important features of the manganites [1–3]. Due to the strong competition between the Jahn–Teller effects, and super-exchange and double-exchange interactions underlying the CO transition, large collective structural distortions and essential electronic property changes always accompany the CO transition. For example, the appearance of a band gap of about 0.3–0.7 eV upon the CO transition has been directly observed for charge-ordered  $\text{Nd}_{0.5}\text{Sr}_{0.5}\text{MnO}_3$  and  $\text{Bi}_{0.24}\text{Ca}_{0.76}\text{MnO}_3$  [4, 5].

Unlike the bulk materials, thin films exhibit lattice strains that can strongly affect the physical properties of the manganites [6, 7]. Because of the presence of lattice strain, the CO state in thin films, mostly deposited on (100)-oriented substrates, is severely depressed, and thus most of the previous studies of the CO effects have focused on bulk manganites. Recently, there have been a lot reports showing the possibility of getting stable charge- and orbital-ordered states in  $\text{Bi}_{0.4}\text{Ca}_{0.6}\text{MnO}_3$ ,  $\text{Nd}_{0.5}\text{Sr}_{0.5}\text{MnO}_3$ , and  $\text{Pr}_{0.5}\text{Sr}_{0.5}\text{MnO}_3$  films grown on

<sup>1</sup> Author to whom any correspondence should be addressed.

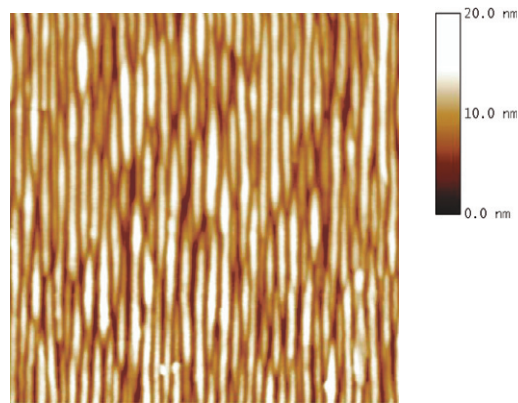


**Figure 1.** Atomic force microscope image of the BCMO film with a scanning size of  $2 \times 2 \mu\text{m}^2$ . (This figure is in colour only in the electronic version)

(110)-oriented  $\text{SrTiO}_3$  substrates [8, 9]. These results make possible further study on the CO effects in manganite films.

As mentioned above, a direct effect of the CO transition is on the electronic structure, and thus the transport behavior of the manganite. Hall effects can provide key information on charge carriers, including their type, density and mobility, which are necessary for elucidating the transport mechanism in charge-ordered manganites. However, the influence of the CO transition on the Hall effect has not been fully explored for the manganite. Nearly all of the previous studies on the Hall effect were performed for the manganite without the CO transition, even for the  $\text{Nd}_{0.5}\text{Sr}_{0.5}\text{MnO}_3$  and  $\text{Pr}_{0.5}\text{Sr}_{0.5}\text{MnO}_3$  films that have a strongly charge-ordered bulk counterpart [10]. The only relevant work may be that of Katsufuji *et al* for  $\text{La}_{2-x}\text{Sr}_x\text{NiO}_4$ , a two-dimensional nickelate [11]. Thus, a systematic investigation on the Hall effect across the CO transition is obviously worthwhile.

One typical charge- and orbital-ordered manganite is  $\text{Bi}_{1-x}\text{Ca}_x\text{MnO}_3$ , for which a strong CO has been observed in a broad doping range from  $x = 0.4$  to  $0.82$  [12, 13]. The CO transition in  $\text{Bi}_{1-x}\text{Ca}_x\text{MnO}_3$  takes place against a paramagnetic (PM) background, which makes the accurate determination of the normal Hall resistivity possible. In this letter, we will present a comprehensive study on the Hall effects of the  $\text{Bi}_{0.4}\text{Ca}_{0.6}\text{MnO}_3$  (BCMO) film experiencing a clear CO transition. Special attention has been paid to the Hall effect around the CO transition. The charge carriers are found to be electron-like, and the carrier density exhibits an activation character below  $T_{\text{co}}$  with an activation energy of  $\sim 0.13$  eV. Effects of the carrier mobility and the density on the resistive anomaly around  $T_{\text{co}}$  and the magnetoresistance are also discussed.

The BCMO film was fabricated on a (110)  $\text{SrTiO}_3$  substrate by the pulsed laser ablation technique from a ceramic target with the nominal composition of  $\text{Bi}_{0.4}\text{Ca}_{0.6}\text{MnO}_3$ . During the deposition, the substrate temperature was kept at  $\sim 700^\circ\text{C}$  and the  $\text{O}_2$  pressure at  $\sim 60$  Pa. The film thickness was  $\sim 1500$  Å, determined by a surface profiler. The epitaxial growth of the film was confirmed by a careful x-ray diffraction analysis. The out of plane  $d_{(110)}$  was  $0.2662$  nm, and the full width at half-maximum of the rocking curve was  $0.26^\circ$  for the (110) peak of the film, similar to the values in [9]. It is interesting that the surface morphology of the film, measured by an atomic force microscope, was found to exhibit a ridge-shaped structure aligned in the [001] direction, with an average column width of  $\sim 50$  nm (as shown in figure 1). The root mean square surface roughness was  $\sim 2.6$  nm for a  $2 \times 2 \mu\text{m}^2$  area. This result indicates the presence of a preferred direction for film growth on the (110) substrate.

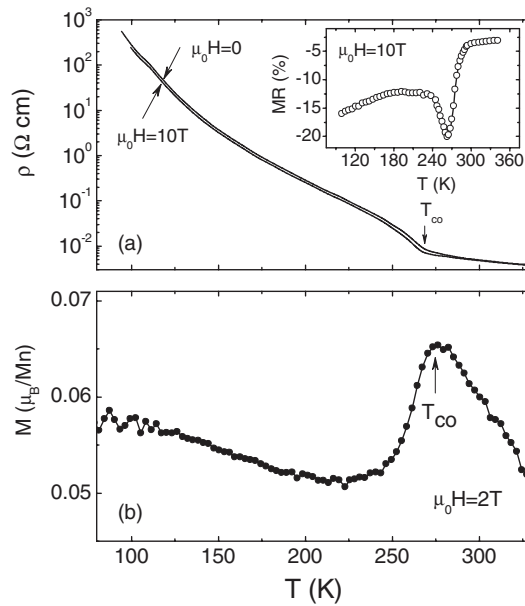


**Figure 2.** (a) Temperature dependence of the resistivity with and without magnetic field and (b) temperature-dependent magnetization recorded under a field of 2 T with the contributions from the substrate subtracted. Upper inset: magnetoresistance as a function of temperature.

Transport and magnetic measurements were performed using a physical property measurement system (PPMS-14h) and a superconducting quantum interference device magnetometer (MPMS-7). To get an accurate determination of the Hall resistivity, the films were patterned, by the conventional photolithographic technique, into a geometry with four terminals. All of the resistive data presented here were measured along the in-plane [001] direction of the film.

Figure 2(a) presents the temperature dependence of the resistivity of the BCMO film. The magnetization recorded under a magnetic field  $H$  of 2 T is shown in figure 2(b), with the contributions of the substrate being subtracted. The film is insulating over the whole temperature range investigated. The obvious resistivity jump on cooling the film through  $\sim 270$  K, accompanied by a magnetization peak, is a signature of the CO transition by analogy with the results for bulk BCMO. The periodic arrangement of  $\text{Mn}^{3+}$  and  $\text{Mn}^{4+}$  localizes charge carriers, thus enhancing the resistivity. Compared with the bulk BCMO case, the CO temperature of the film is significantly low,  $\sim 270$  K for the film and  $\sim 330$  K for the bulk [13], which could be an effect of the lattice strain imposed by substrate. These results are also similar to those previously reported [9].

The CO state of the BCMO film is stable. As also shown by figure 2(a), the CO transition remains essentially unaffected under a field of 10 T, with only a small resistivity decrease. Effects of the CO transition on the MR are obvious (inset in figure 2(a)); the MR exhibits a peak value of  $\sim 20\%$  at  $T_{\text{CO}}$ . The significant enhancement of the MR near the CO transition results from the increase of carrier mobility under a magnetic field as will be seen below.

To get the information about the electronic structure of the BCMO film around the CO transition, the Hall effect was further studied. The Hall resistivity was measured using the PPMS system at various temperatures with the magnetic field up to 10 T. The temperature fluctuation was controlled below 0.01 K during the measurements. An alternating current mode

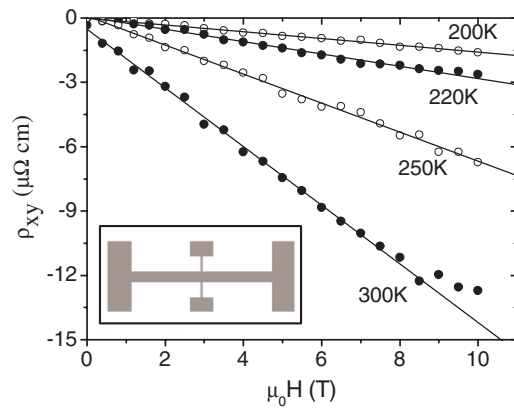


**Figure 3.** Hall resistivity as a function of magnetic field for selected temperatures between 200 and 300 K. Solid lines are guides for the eye. The inset plot is a schematic diagram of the Hall sample.

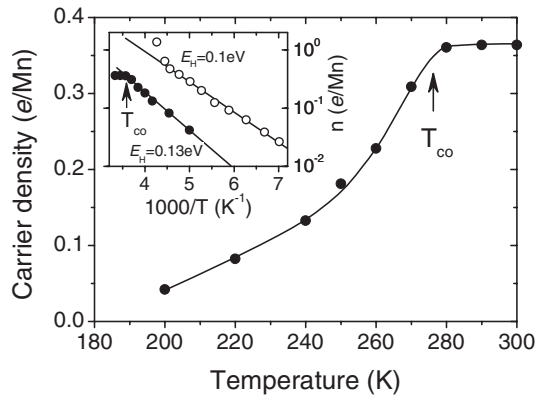


**Figure 4.** Carrier density as a function of temperature. Inset plot: a semi-log plot of carrier density against reciprocal temperature for the BCMO film (solid symbols) and for the  $\text{La}_{2-x}\text{Sr}_x\text{NiO}_4$  single crystal (open symbols). Solid lines are guides for the eye.

was used to eliminate undesired effects arising from, for example, possible thermopower and contact voltage. To remove the offset voltage due to the asymmetry of the Hall terminals or subsisting MR, two voltage signals corresponding to  $H$  and  $-H$  should be measured. For the present experiment, the transverse voltage under the field of  $-H$  was obtained by rotating the sample by  $180^\circ$  while the magnetic field was kept unchanged. The transverse Hall voltage was half of the sum of these two signals.

Figure 3 shows the Hall resistivity as a function of magnetic field for selected temperatures between 200 and 300 K. The Hall resistivity is found to increase linearly with magnetic field with a negative  $\rho_{xy}-\mu_0 H$  slope over the whole temperature range investigated ( $\rho_{xy}$ : transverse resistivity), indicating the electron-like character of the charge carriers as expected from the nominal doping level. The Hall coefficient  $R_H$  can be obtained on the basis of the relation  $\rho_{xy} = R_H \mu_0 H$ , and the deduced carrier density is  $n = -1/eR_H$ , where  $e$  is the electron charge. Figure 4 shows the carrier density as a function of temperature.  $n$  is  $\sim 0.36$  electrons/Mn in the temperature range above  $T_{CO}$ , essentially independent of temperature. It is close to 0.4 electrons/Mn, a value expected from the nominal doping level. The CO transition triggers

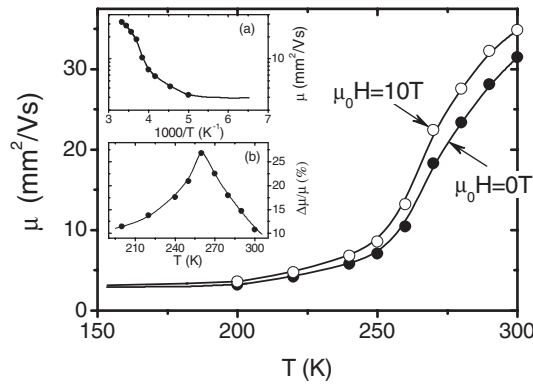


**Figure 5.** Mobility of charge carriers as a function of temperature and magnetic field. Inset (a) mobility as a function of reciprocal temperature. Inset (b) relative mobility change under the field of 10 T.

a decrease of the carrier density. The change of  $n$  is rapid near  $T_{\text{co}}$  and smooth well below  $T_{\text{co}}$ , and a density of  $\sim 0.04$  electrons/Mn is obtained at the temperature of 200 K. The Hall signals could not be measured below 200 K because of the poor signal/noise ratio. It is a reasonable inference that the carrier density could be extremely low at much lower temperatures.

The Hall mobility can be obtained from the simple relation  $\mu = -R_{\text{H}}/\rho_{\text{xx}}$ . As shown in figure 5, the carrier mobility is  $\sim 32 \text{ mm}^2 \text{ V}^{-1} \text{ s}^{-1}$  at 300 K, and reduces monotonically to  $\sim 7 \text{ mm}^2 \text{ V}^{-1} \text{ s}^{-1}$  as the temperature decreases from 300 to 250 K. Further decrease leads to an obviously slow change of  $\mu$ , and a mobility of  $\sim 3 \text{ mm}^2 \text{ V}^{-1} \text{ s}^{-1}$  is obtained at  $\sim 200$  K. The considerably inclined  $\mu$ - $T$  slope in the temperature range 260–280 K manifests the depression of carrier mobility by the CO transition. As expected, the mobility is obviously low in the charge-ordered state.

A further analysis reveals the activated character of the charge carriers. As shown by the inset plot in figure 4, a growth of the carrier density with the increase of the temperature following the formula  $n \propto \exp(-E_{\text{H}}/k_{\text{B}}T)$  appears below  $T_{\text{co}}$ , with the activation energy of  $E_{\text{H}} \approx 0.13$  eV. We analyzed the data for  $\text{La}_{2-x}\text{Sr}_x\text{NiO}_4$  for the hole concentration of  $x = 0.3$  and observed an  $n$ - $T$  relation similar to that for the BCMO film, except for a lower activation energy  $E_{\text{H}} \approx 0.1$  eV (open symbols in the inset of figure 4). This result indicates that the exponential behavior of the temperature-dependent carrier density below  $T_{\text{co}}$  could be a general feature of charge-ordered perovskites.

Activated behaviors have been observed previously for both the Hall coefficient and Hall mobility, and were ascribed to small polaron hopping [14]. In order to analyze the temperature dependence of the Hall mobility over a wider temperature range, the  $n = n_0 \exp(-E_{\text{H}}/k_{\text{B}}T)$  relation was extrapolated down to 160 K, considering similar intrinsic conducting behavior between 160 K and  $T_{\text{co}}$ . No obvious activated signature is observed in the temperature-dependent Hall mobility below  $T_{\text{co}}$ , though  $\mu(T)$  displays a smooth increase with  $T$  (inset (a) of figure 5). This result indicates that the transport behavior of the charge-ordered manganite may be different from a simple adiabatic small polaron hopping. Therefore, the exponential variation of  $n$  with  $T$  in the BCMO film may be of a different origin, probably a result of the carrier excitation from the Fermi level to the conduction band. It is rather interesting that the temperature dependence of  $n$  would indicate the opening of a band gap of  $\sim 0.26$  eV upon the CO transition, nearly the value obtained from scanning tunneling spectroscopy measurements [4, 5], following the semiconductor theoretical form  $n \propto \exp(-E_{\text{H}}/k_{\text{B}}T)$  [15].

It is obvious that a deep insight into the underlying mechanism for this phenomenon requires further work.

Mobility under magnetic field can also be obtained. It shows a considerable increase, and the largest relative change appears near 260 K, where the strongest MR effects occur (inset (b) of figure 5). These results reveal the predominant role of the field-induced mobility change, rather than carrier density, in affecting the MR of the BCMO film around the CO transition. This is a conclusion similar to that obtained for the PM–FM transition in optimally doped manganite  $\text{La}_{0.67}\text{Ca}_{0.33}\text{MnO}_3$  [16]. Unlike the MR case, reduction in both the carrier density and mobility could be responsible for the resistivity jump near  $T_{\text{co}}$ .

In summary, charge-ordered  $\text{Bi}_{0.4}\text{Ca}_{0.6}\text{MnO}_3$  films have been prepared by growing the films on (110)  $\text{SrTiO}_3$  substrates, and their transport properties were experimentally studied. Special attention has been paid to the Hall effect around the charge-ordering (CO) transition. The charge carriers are found to be electron-like and the carrier density exhibits a significant decrease upon the CO transition following  $n \propto \exp(-E_{\text{H}}/k_{\text{B}}T)$  below  $T_{\text{co}}$ , with an activation energy of  $\sim 0.13$  eV. In contrast, no obvious signatures of thermal activation for Hall mobility were observed. Meanwhile, the sharp enhancement of the magnetoresistance near the CO transition is found to result from the increase of the carrier mobility under magnetic field.

This work was supported by the National Natural Science Foundation of China and the National Basic Research of China.

## References

- [1] Tokura Y and Nagaosa N 2000 *Science* **288** 462
- [2] Ziese M 2002 *Rep. Prog. Phys.* **65** 143
- [3] Rao C N R, Arulraj A, Cheetham A K and Raveau B 2000 *J. Phys.: Condens. Matter* **12** R83
- [4] Renner C, Aeppli G, Kim B G, Soh Y and Cheong S W 2002 *Nature* **416** 518  
Renner C, Aeppli G and Ronnow H M 2005 *Mater. Sci. Eng. C* **25** 775
- [5] Biswas A, Raychaudhuri A K, Mahendiran R, Guha A, Mahesh R and Rao C N R 1997 *J. Phys.: Condens. Matter* **9** L355  
Biswas A, Arulraj A, Raychaudhuri A K and Rao C N R 2000 *J. Phys.: Condens. Matter* **12** L101
- [6] Millis A J 1998 *Nature* **392** 147
- [7] Prellier W, Lecoeur P and Mercey B 2001 *J. Phys.: Condens. Matter* **13** R915
- [8] Nakamura M, Ogimoto Y, Tamaru H, Izumi M and Miyano K 2005 *Appl. Phys. Lett.* **86** 182504  
Ogimoto Y, Takabo N, Nakamura M, Tamaru H, Izumi M and Miyano K 2005 *Appl. Phys. Lett.* **86** 112513  
Wakabayashi Y, Bizen D, Nakao H, Murakami Y, Nakamura M, Ogimoto Y, Miyano K and Sawa H 2006 *Phys. Rev. Lett.* **96** 017202
- [9] Kim D H, Christen H M, Varela M, Lee H N and Lowndes D H 2006 *Appl. Phys. Lett.* **88** 202503
- [10] Wagner P, Gordon I, Vantomme A, Dierickx D, Vanbael M J, Moshchalkov V V and Bruynseraede Y 1998 *Europhys. Lett.* **41** 49  
Wagner P, Mazilu D, Trappeniers L, Moshchalkov V V and Bruynseraede Y 1997 *Phys. Rev. B* **55** R14721
- [11] Katsufuji T, Tanabe T, Ishikawa T, Yamanouchi S, Tokura Y, Kakeshita T, Kajimoto R and Yoshizawa H 1999 *Phys. Rev. B* **60** R5097
- [12] Bao W, Axe J D, Chen C H and Cheong S W 1997 *Phys. Rev. Lett.* **78** 543
- [13] Woo H, Tyson T A, Croft M, Cheong S W and Woicik J C 2001 *Phys. Rev. B* **63** 134412
- [14] Salamon M B and Jaime M 2001 *Rev. Mod. Phys.* **73** 583
- [15] Sze S M 1981 *Physics of Semiconductor Devices* 2nd edn (New York: Wiley) p 27
- [16] Jakob G, Martin F, Westerburg W and Adrian H 1998 *Phys. Rev. B* **57** 10252